EVOLUTION OF AIRFOILS FOR SAILPLANES

By K. H. Horstmann, German Aerospace Center, Braunschweig
L. M. M. Boermans, Delft University of Technology, Netherlands

ABSTRACT

About 110 years ago O. Lilienthal built his gliders with cambered plate wings which were stiffened out by a plenty of strut wires. Analysis of this type of airfoils show their narrow range of angles of attack and their rapid loss of lift at stall conditions. The development of the thick airfoils of the Göttingen series led to the construction of the Vampyr with a strut free wing and a torsion leading edge box. The quality of the surface and the maximum thickness close to the leading edge did not allow reasonable extent of laminar flow. The big advantages of laminar flow airfoils have been discovered in the late thirties and have been systematically investigated by the NACA. But only the combination of an airfoil designed for laminar flow and the excellent surface quality of a sandwich construction of glass fibre reinforced plastics and solid foam made the big success of laminar airfoils for sailplanes possible. This is shown by way of the example of the Ka 6 and the Phönix. Examples of typical airfoils demonstrate further developments: Airfoils without and with flaps; problem of laminar separation bubbles, use of destabilisation zones and use of turbulators. An attempt to assess future possibilities for performance improvements of sailplanes closed the paper.

INTRODUCTION

After several attempts of flying during the second half of the 19th century Otto Lilienthal was the first who succeeded in well observed and documented flights during the last decade of that century. From these glides over 25 m in the summer of 1891 to the performances of modern sailplanes of today allowing to fly distances of 3000 km within one day only driven by the power of the sun, a huge technical development on all aspects of flying but also a considerable mental development of the pilots have happened.

This technical development took place in countless number of small and bigger steps of many different disciplines. All steps are strongly depending on previous ones. A new technology or physical understanding in one discipline allowed advantages in other disciplines.

In particular this is valid for the development of wing sections of sailplanes: for example the design of thick airfoils lead to the cantilever mono wing with torsion leading edge box of the Vampyr; the high quality of a sandwich structure surface allowed the use of laminar flow airfoils and the advantageous airfoil design methods of R. Eppler and M. Drela enable an optimum adaptation of airfoils on the design flight envelope of sailplanes.

EARLY AIRFOILS

For the people up to the 19th century the nature provides the example of flying. They observed the flying of insects and birds and they saw foldable wings of chitine or with feathers being all very thin as it is useful for the low Reynolds numbers. For the very low Reynolds numbers of insects the surface even must not be smooth or not cambered normal to flow direction. The feather wings of birds however are relatively smooth, they are cambered, but they are also thin. No wonder that most of the early airfoils stamped by nature show thin flat airfoils. Otto Lilienthal found by means of simple aerodynamic tests in a rotating test rig that the lifting component in relation to the "hampering" component (now called drag component) is very favourable for a wing slightly cambered normal to flow

Fig. 1: Lilienthal with his "Normal Sailing Apparatus" from 1894 achieving distances of 80 m from a height of about 15 m

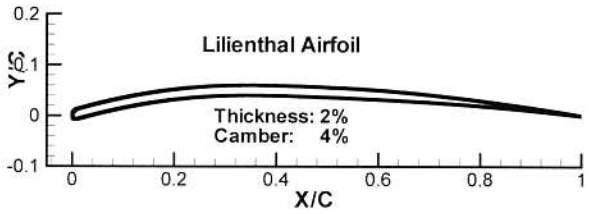

Fig. 2: Approximate shape of a Lilienthal glider Airfoil

direction. This was the origin of the airfoil polar, also called Lilienthal Polar. By the observation of bird flying and by means of numbers of physical tests Lilienthal found geometry and structure of the first apparatus enabling him to perform gliding flights. With this glider called simply "Glider No. 3" he succeeded in performing glides up to a distance of 25 m during the summer of 1891. Figure 1 gives an impression of this apparatus, taken from [1]. The wing is like a cambered plate with a thickness of about 2% containing round wooden laths in span and cord direction

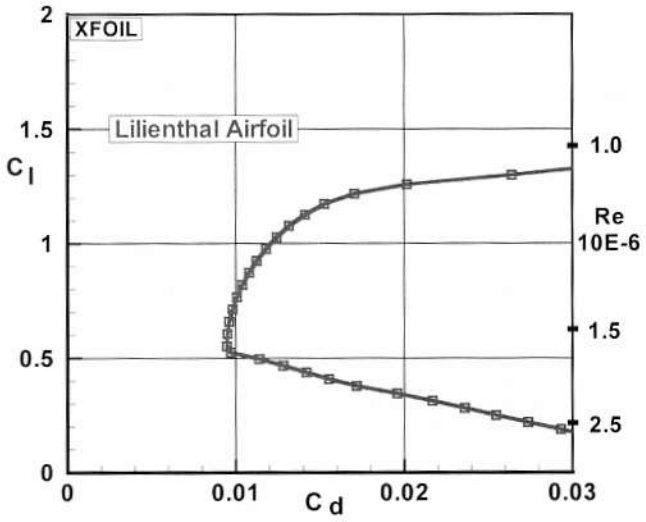

Fig. 3: Calculated drag coefficient characteristic of a typical Lilienthal Airfoil (Thickness: 2%, Camber: 5%)

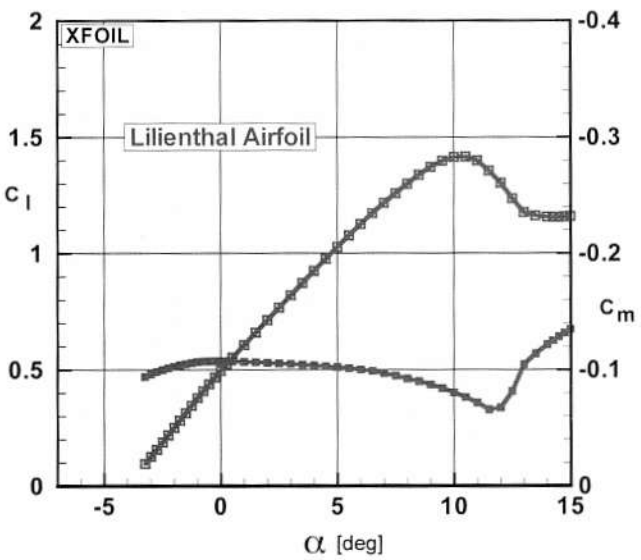

Fig. 4: Lift and moment coefficient behaviour of a typical Lilienthal Airfoil (Thickness: 2%, Camber: 5%)

stiffened out by thin wires. An example airfoil of this type is shown in figures 2.

The aerodynamic characteristics of this airfoil are shown in figures 3 and 4. As in several of the following figures the performance of an airfoil is characterised by the drag coefficient cd versus the lift coefficient cl (figure 3) and by lift coefficient cl and moment coefficient cm versus angle of attack (figure 4). For most of the airfoils discussed in this paper these characteristic parameters have been determined by means of the XFOIL code [2] or of the Eppler airfoil code [3], two well known numerical methods for airfoil analysis and design.

An important parameter representing the influence of surface friction on an airfoil is the Reynolds number defined by:

$$\mathrm{Re} = (V_\infty * l)/\nu$$

with the flow velocity V∞ , the local chord length l and the kinematic viscosity _. At flight conditions the Reynolds number is decreasing proportional to (1/cl)0.5 with increasing lift coefficient. Consequently for most of the numerical results the Reynolds number chosen depends on the lift coefficient following the equation

$$\mathrm{Re}*\sqrt{c_l} = \frac{1}{\nu}\left[\frac{2\cdot m\cdot g}{\rho\cdot\Lambda}\right]^{1/2} = 1.2\cdot 10^6$$

with the mass m, the density ¡, the aspect ratio õ, and the gravity acceleration g. The lift dependent Reynolds num-

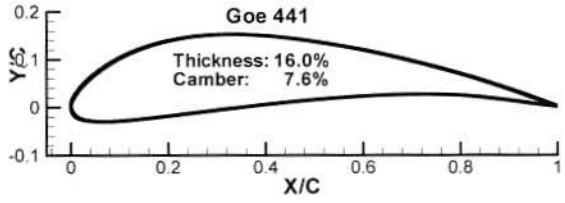

Fig. 6: Shape of the airfoil Goe 441 of the Vampyr

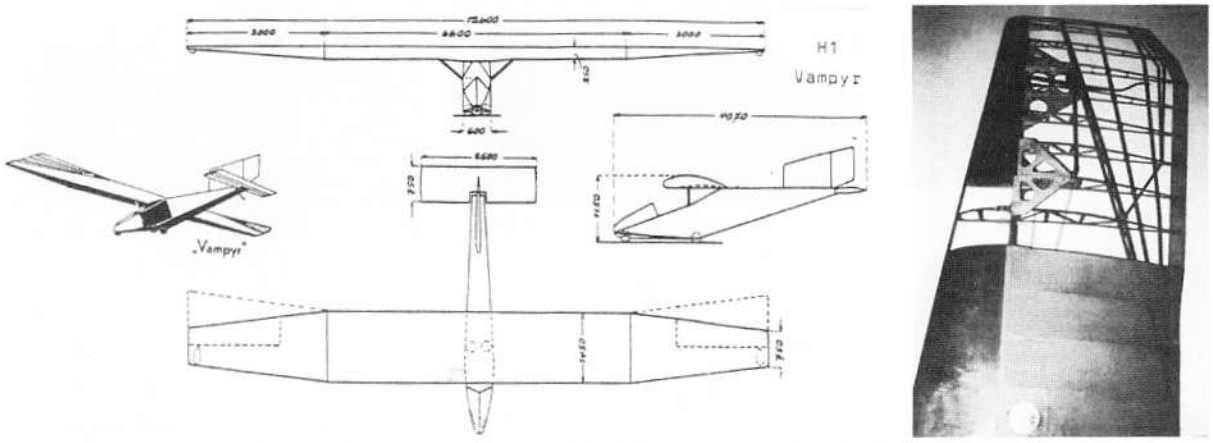

Fig. 5: Top view and insight into the structure of the Vampyr, showing the leading edge torsion box

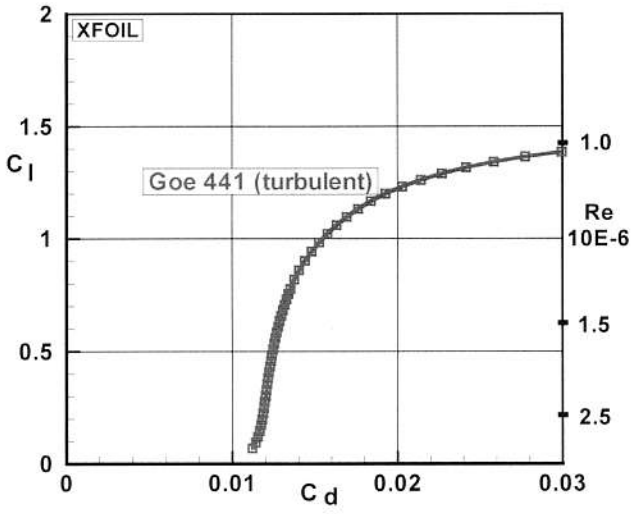

Fig. 7: Calculated drag coefficient characteristics of the Goe 441 airfoil for fully turbulent boundary layer

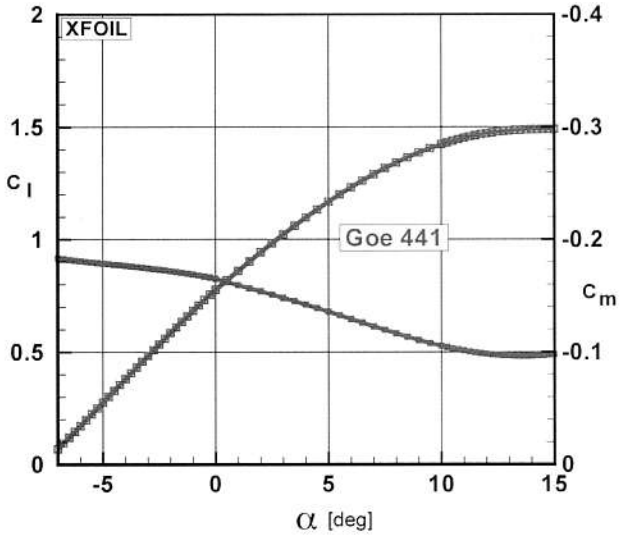

Fig. 8: Calculated lift and moment coefficient behaviour of the Göttingen airfoil Gö 441 for fully turbulent boundary layer

ber is marked in the cl-cd plot for the three values Re=1.0, 1.5 and 2.5.

The drag polar of the Lilienthal airfoil in figure 3 has a limited range of lift coefficients with low drag. Considering the extremely low thickness with the very small leading edge radius the usable range of lift coefficients is surprisingly large. But the strong lift break down at angles of attack (AoA) above 15° visible in figure 4 is a typical behaviour for this type of airfoil and may cause in flight asymmetrical flow separation accompanied by large bank angles. The rapidly increasing drag coefficients at lift coefficients below cl = 0.5 clearly indicates a flow separation on the lower side of the airfoil. The moment coefficient is nearly not influenced by the flow separation. The slope is slightly destabilising in the linear range but shows a strong nose down moment increase in the stall region which is very helpful for lateral control in particular for the Lilienthal glider being controlled by shifting the centre of gravity by means of the pilot body.

Lilienthals problems in particular of bank control have been overcome by the Wright brothers. They introduced the control of the moment balance for all three axis by the aerodynamic means of rudders.

A big step on the way to the modern sailplanes represents the Vampyr built 1921 by the Academics Flying Group (Akaflieg) Hanover, a student group at the Technical University of Hannover. Many components of modern sailplanes have already been applied: three axis aerodynamic balance control, covered fuselage, cantilever mono wing, single spar for wing bending moments and a closed leading edge box for torsion stiffness, shown in figure 5. Such a structural design needs a completely different airfoil than a Lilienthal glider. The Airfoil Gö 441, see [4], used for the Vampyr is shown in figure 6. It has a moderate thickness of 16% at about 25% of chord, and a high camber of 7.6% both typically for fully turbulent airfoils. The drag, lift and moment characteristics of this airfoil displayed in figures 7 and 8 for fully turbulent flow, show a much more even behavior of pitching moment, lift, and drag characteristics than the Lilienthal airfoil type in figures 3 and 4.

LAMINAR AIRFOILS

Until the late Thirties nearly exclusively Göttinger airfoils have been used for sailplane design. The Gö 441 derived from a Joukowsky airfoil have been further

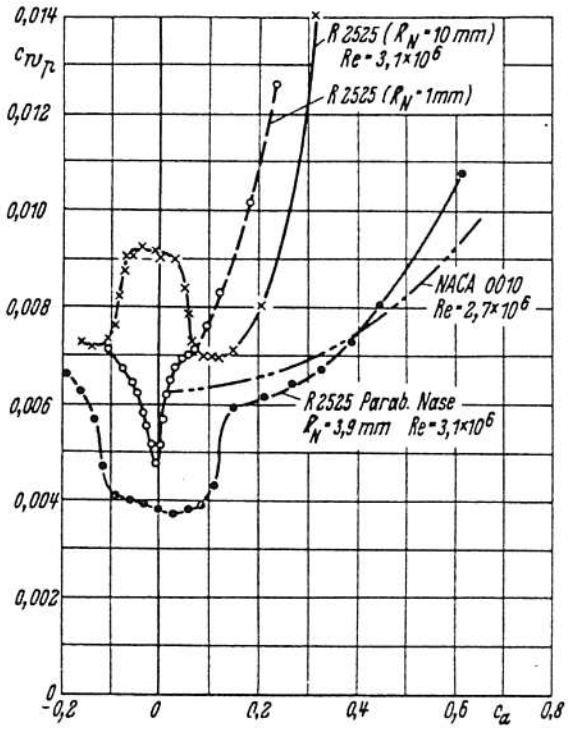

Fig. 9: Wind tunnel tests of an airfoil with large extent of laminar flow in 1938 by H Doetsch [3]

improved and the airfoils Gö 532, Gö 535 and Gö 549 have been used for the wings of a large number of sailplanes being developed between 1921 and 1942.

All these airfoils have been developed for turbulent boundary layer. The drag of airfoils with a reasonable share of laminar boundary layer is half of the value of an airfoil with fully turbulent boundary layer. But the quality of the surface of original wings and of wind tunnel models was for a long time not good enough to allow large extents of laminar flow. Early wind tunnel measurements of an airfoil with a large extent of laminar flow on both sides have been performed by H. Doetsch in 1938 [5]. As shown in figure 9, Doetsch measured drag coefficients below 0.004 at a Reynolds number of 3.1 Million with a transition location at 74% of chord.

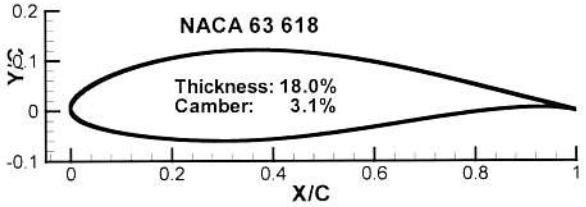

Fig. 10: Shape of the NACA airfoil NACA 63_3 618 of the of the Ka 6

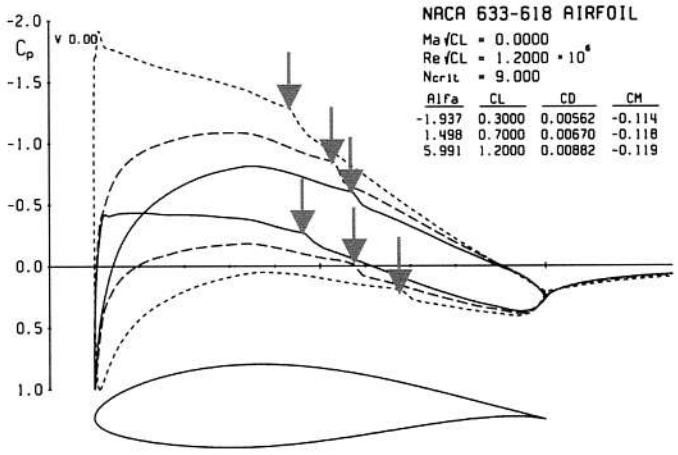

Fig. 11:Calculated pressure distributions of the NACA airfoil NACA 63_3 618

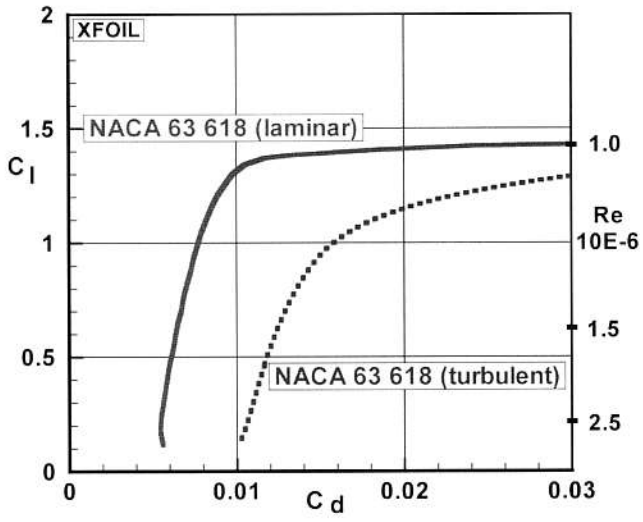

Fig.12: Calculated drag coefficient characteristics for laminar and turbulent boundary layer of the NACA 63_3 618 airfoil

Systematically laminar airfoil have been investigated by the NACA. The application of the famous NACA-6-series airfoils being developed since the early forties, see [6], led to first experiences with sailplanes with laminar flow wings in the late forties and the early fifties. The wings require an extremely low surface roughness and a very accurate shape of the airfoil contour. This was difficult to achieve with the wooden kind of structure of the early fifties. Further due to weight the torsion D-box was limited to less than the first 30% of wing chord followed by a covering, clearly terminating the laminar boundary layer.

One of the most successful sailplane of that time was the Ka 6. For the inner part of the wing the NACA 633 618 airfoil was used, shown in figure 10. At first sight its shape looks already very similar to modern airfoils. The pressure distributions of this airfoil in figure 11 is given as in all following figures showing pressure distributions at lift coefficients representing cruise condition (cl = 0.3), maximum lift over drag, LoD (cl = 0.7) and climb (cl = 1.2). The transition locations are marked by arrows. Natural transition on both sides occur between 45% and 70%. The wooden and covering surfaces induced premature transition. The drag polars for laminar boundary layer and for fully turbulent boundary layer in figure 12 show the large difference of drag between both. For fully turbulent flow the drag is nearly twice as high as for laminar flow. Thus the potential of this airfoil with respect to flight performance could not be fully used with wooden sailplanes of that time.

This situation was completely changed when in the late fifties a new type of construction came up: the technology of the fiberglass composite structure. It allows to manufacture an accurate shape of the wing with a smooth surface for the whole wing. R. Eppler was the first using the potential of this technology when he designed the "Phoenix" in 1957, figure 13.

The contour of the Phoenix airfoil EC 86(-3)-914 is presented in figure 14. Conspicuous and a characteristic of most of Epplers airfoils is the high camber at the rear of the airfoil. The design philosophy becomes evident by means of the pressure distributions of figure 15. At lift coefficients for maximum LoD both sides of the airfoil show large extents of laminar flow regions. In particular the laminar flow on the upper surface is extended downstream to nearly 90% of chord. At the lower lift coefficients for straight forward flight the transition on the upper surface remains nearly constant whereas transition on the lower surface moves continuously upstream. At climbing with higher lift coefficients just the opposite happened: the extent of lami-

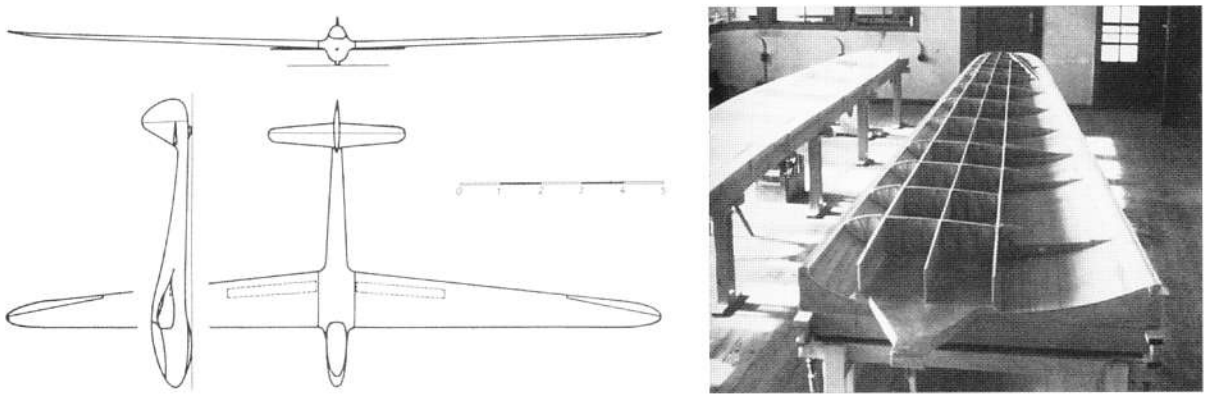

Fig. 13: Top view and insight into the wing structure of the Phoenix, showing the wing upper side in the negative mould

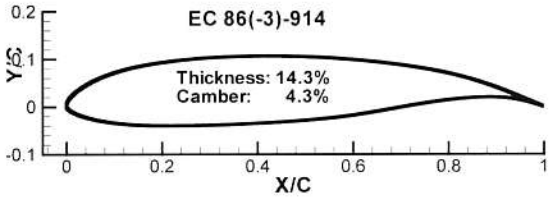

Fig. 14: Shape of the Eppler airfoil EC 86(-3)-914 used for the Phoenix

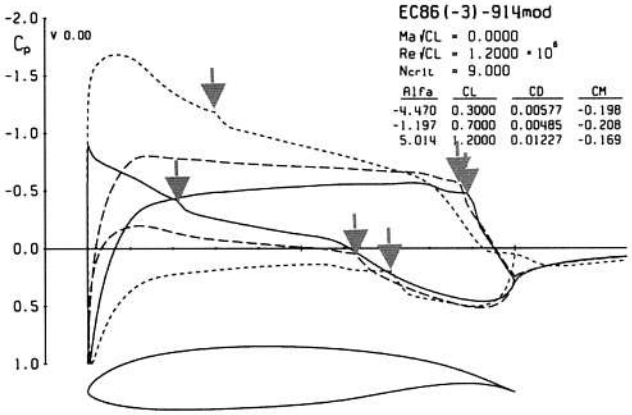

Fig. 15:Calculated pressure distributions of the Eppler airfoil EC 86(-3)-914

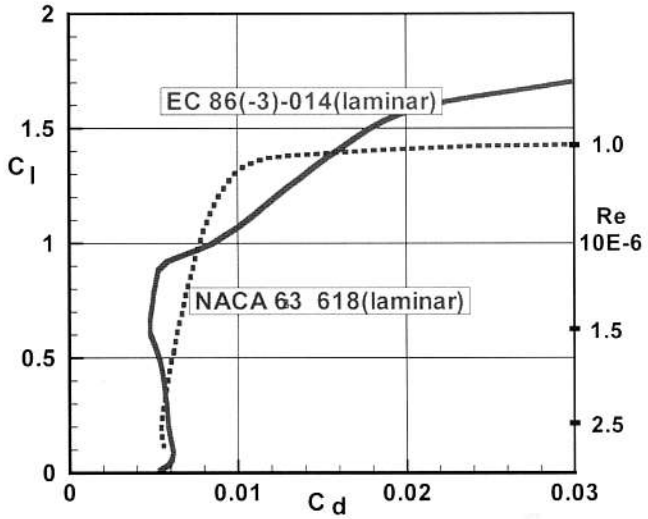

Fig.16: Calculated drag coefficient characteristics of the Phoenix airfoil EC 86(-3)-914 and of the Ka 6 airfoil NACA 63_3 618

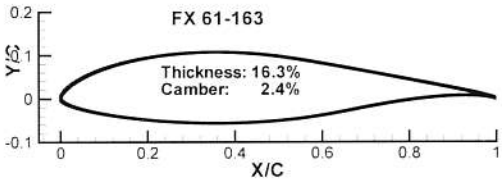

Fig. 17: Shape of the airfoil FX 61-163 (ASW 15, Elfe S3)

nar flow on the lower side remains constant whereas the transition on the upper side moves considerably fast upstream. The drag polar in figure 16 reflects this behaviour of the laminar flow. The very low drag at lift coefficients from 0.6 to 0.9 is a result of the long extent of laminar flow on both sides of the airfoil. At higher and lower lift coefficient the drag is increasing due to reduced extent of laminar flow on the upper respectively on the lower side of the airfoil. The high maximum lift coefficient is a result of the large curvature on the rear of the upper airfoil side which is fixing the flow separation within the high curvature region up to large angles of attack.

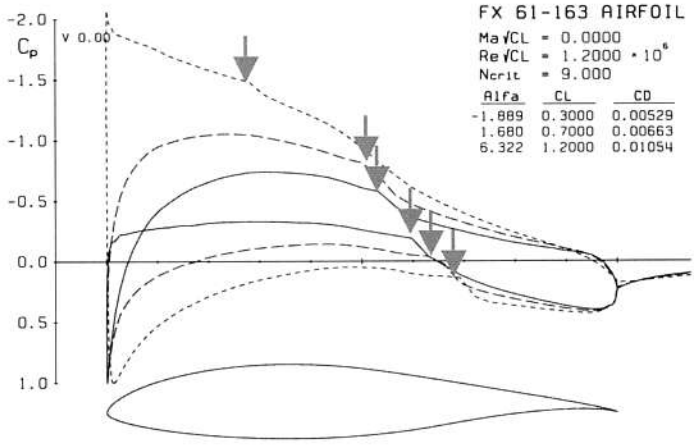

Fig. 18: Calculated pressure distributions of the Wortmann airfoil FX 61-163

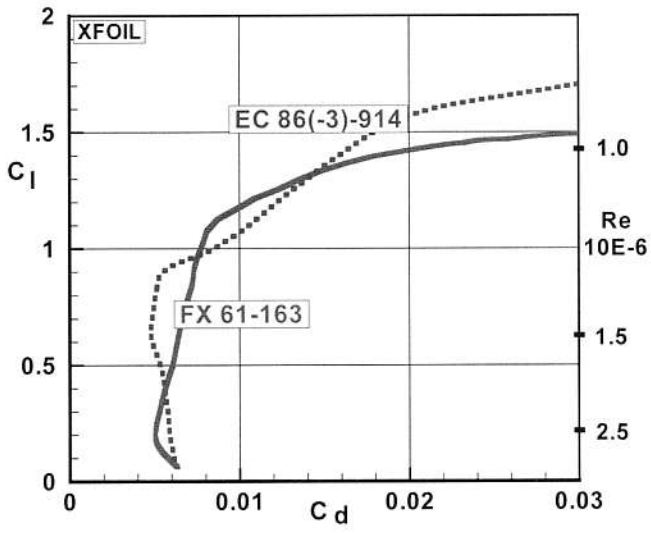

Fig.19: Calculated drag coefficient characteristics for of the airfoils FX 61-163 and EC 86(-3)-914

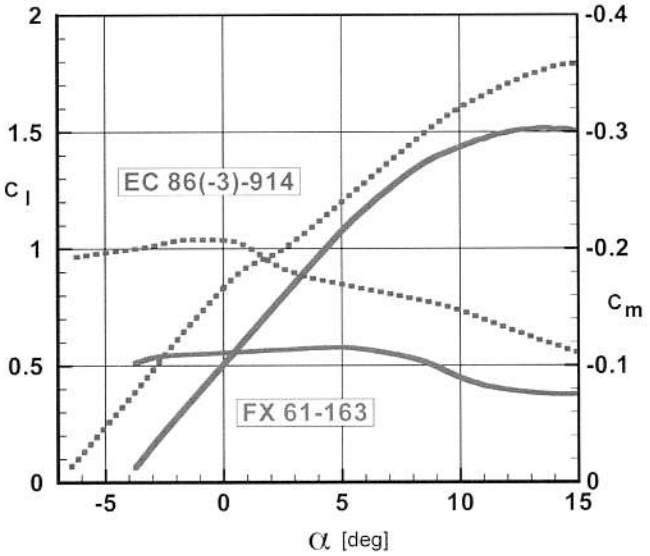

Fig. 20: Calculated lift and moment coefficient behaviour of the airfoils FX 61-163 and EC 86(-3)-914

A very successful work on airfoil design and testing over three decades have been performed by F. X. Wortmann and D. Althaus, see [7]. One of their first well known airfoils is the FX 61-163, figure 17, designed in 1961. Already the shape of this airfoil in comparison to the Phönix airfoil in figure 14 clarifies a different design philosophy. In figure 18 the pressure distributions with transition locations marked by arrows show a moderate extent of laminar flow on both sides of the airfoil. In particular on the lower side at cruise, cl = 0.3, the extent of laminar flow could be kept far downstream. The result of this philosophy is a very even distribution of drag coefficients, shown in figure 19. At cruise condition a clear advantage is visible but at medium lift coefficients the higher drag compared to the Phönix airfoil will result in a reduced maximum glide ratio. Typical differences between both airfoils are also visible in figure 20. The rear located maximum camber of the Phönix airfoil leads, as discussed above, to a considerably higher maximum lift coefficient than of the FX 61-163 but also to a moment coefficient which is twice as high as that of the FX

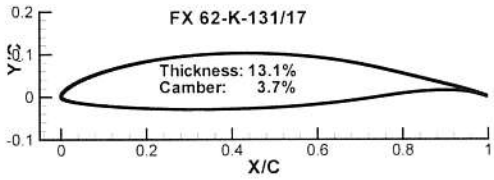

Fig. 21: Shape of the airfoil FX 62-K-131/17 (D36)

61-163. The difference in slope of upper and lower part of the lift curve of the Phönix airfoil indicates small trailing edge separations above lift coefficients of cl = 1, which explains the strong drag increase near cl = 1 in figures 16 and 20.

LAMINAR AIRFOILS WITH FLAP

Low drag for a large range of lift coefficients is the main objectives of airfoil design for sailplanes. With respect to the flow physics these objectives are unfortunately contrary directed: the larger the thickness ratio of an airfoil the larger the lift coefficient range of low drag but the higher the drag itself. The effect of this behaviour can be avoided by use of a simple camber flap. By means of a positive flap deflection the laminar drag bucket is shifted to higher values of lift coefficients in case of positive deflections and vice versa. Thus, it is possible to design rather thin airfoils with large extent of laminar flow and low drag but only for a small range of lift coefficients. The adaptation of the wing for cruise , best LoD, or climb has then to be done by setting the flap by the pilot.

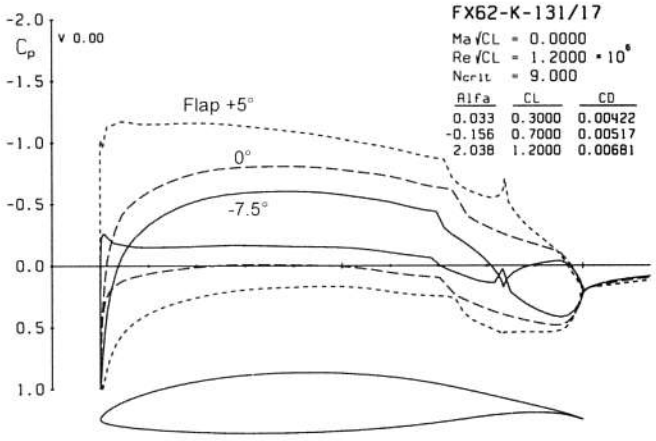

Fig. 22: Calculated pressure distributions of the Wortmann airfoil FX 62-K-131/17

The Wortmann airfoil FX 62-K-131/17, figure 21, is one of the early camber flap airfoils used at first for the D 36 of the Academic Flight Group of Darmstadt and later with slight modifications in many other sailplanes. The pressure distributions for the same lift coefficients as before but with

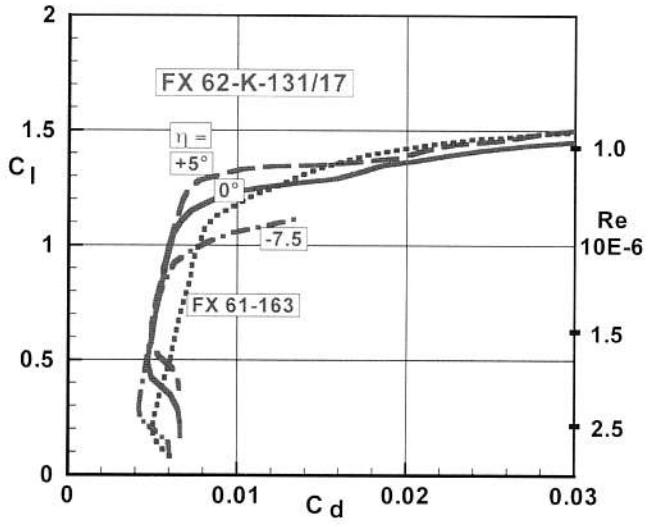

Fig.23: Calculated drag coefficient characteristics of the Wortmann airfoils FX 62-K-131/17 and FX 61-163

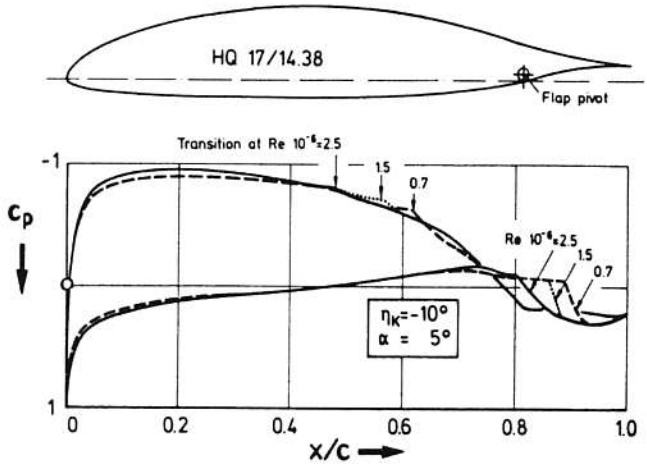

Fig. 25: Appearance of laminar separation bubbles in the pressure distribution of the airfoil HQ 17/14.38 for different Reynolds number (Measurement TU Delft)

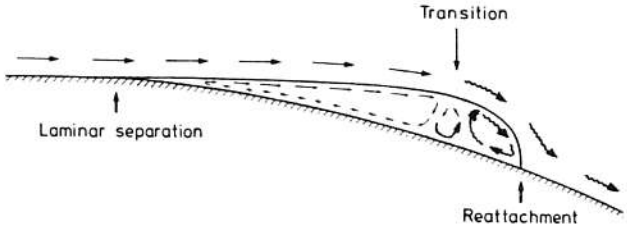

Fig. 24: Model of a laminar separation bubble on a wing surface

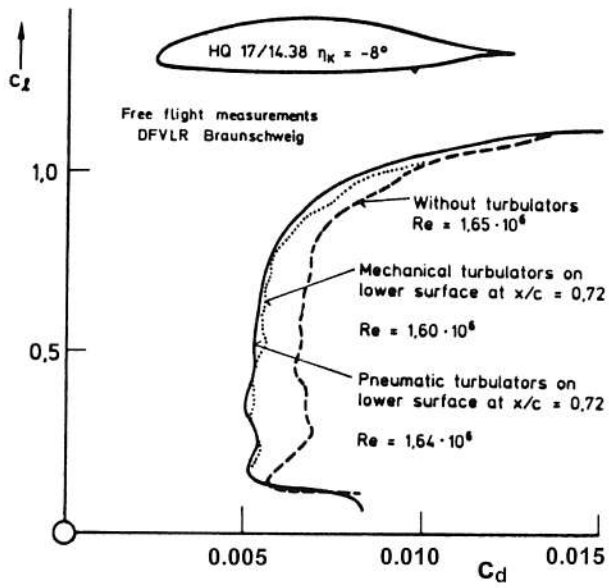

Fig. 26: Influence of transition tripping by means of pneumatic turbulators and zick-zack tape on airfoil drag coefficient

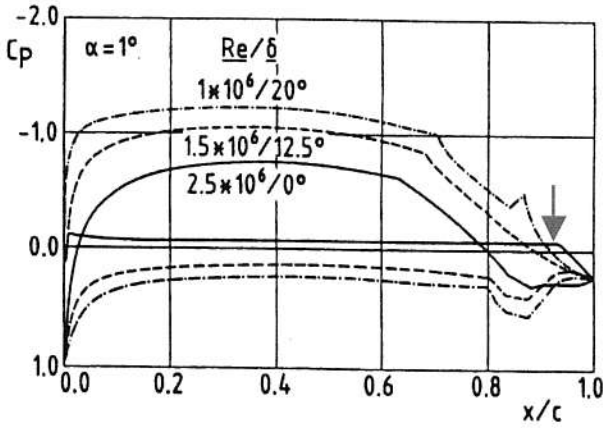

Fig. 27: Airfoil DU89-134/14 designed for use of pneumatic turbulators on the lower side of the flap (see arrow), (Measurement TU Delft)

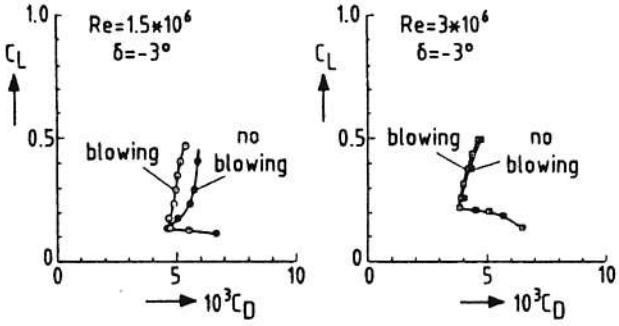

Fig. 28: Influence of pneumatic turbulators on the drag coefficient of the airfoil DU89-134/14 (Measurement TU Delft)

corresponding flap deflections and with marks at transition locations in figure 22 show large extents of laminar flow on both airfoil sides even slightly downstream of 70% of chord length. Figure 23 shows very nicely the typical effect of flap deflection on the laminar drag bucket and it also shows the very low drag of this airfoil with values below 0.005 for cruise conditions.

One of the crucial points of airfoil design for sailplane is the avoidance of drag producing laminar separation bubbles. The principle of a separation bubble is sketched in figure 24 taken from [8]. Caused by the ability of laminar boundary layer, to overcome only weak adverse pressure gradients, the flow tends to separate very easily. The separated flow becomes turbulent and the large energy transfer across the flow direction results in a reattachment of the flow. Extent and drag of the separation bubble depends on the Reynolds number, the destabilisation of the laminar flow in advance of the separation, and on the shape of the contour in the bubble region. Figure 25 shows the appearance of separation bubbles at lower side pressure distributions of the DLR airfoil HQ 17/14.38 for different Reynolds numbers.

Decreasing Reynolds number results in increasing extent of the bubble. At the same Reynolds numbers the pressure distributions of the upper side indicate only very small separation bubbles or even laminar-turbulent transition. The reason for this different behaviour is the slight adverse pressure gradient in front of the bubbles. This "destabilisation zone" forces the laminar boundary layer to an earlier transition thus reducing the extent of the separation bubble. The destabilisation zone has been used by Wortmann and Eppler for most of their sailplane airfoils.

The experience with airfoil design for sailplane clearly shows that it is not possible to avoid the laminar separation bubbles for the whole Reynolds number range of sailplane airfoils. A way out is to force transition by turbulators. Mechanical turbulators like a tape with a row of small bumps and zick-zack-tape with a saw tooth type of shape at the front and the rear edge are successfully investigated in different wind tunnels and in flight. Very efficient proved to be pneumatic turbulators, first investigated at DLR in Braunschweig, see [9]. Blowing, driven by stagnation pressure, through small holes (0.6 mm diameter, 20 mm spacing) in the wing surface induce turbulent wedges and form a transition front slightly downstream of the holes. Figure 26 shows the remarkable difference of drag polars with and without turbulators for the DLR airfoil HQ 17/14.38.

The airfoil DU89-134/14 of the Delft University, see [10], is designed for the use of pneumatic turbulators on the lower side of the flap as visible in figure 27. At cruise design condition the pressure is nearly constant on the lower side up to 92% of chord. Instead of a destabilisation zone pneumatic turbulators avoid laminar separation, which, if it occurs, probably would not reattach again because the trailing edge is very close to the separation line. Separated flow on the lower side at the trailing edge is really unwanted because it could remarkably influence lift and drag coefficients. The effect of blowing for this airfoil is shown in figure 28. At a Reynolds number of 1.5 Million the drag coefficient is reduced up to about 20% by blowing, whereas at 3.0 Million nearly no difference can be stated.

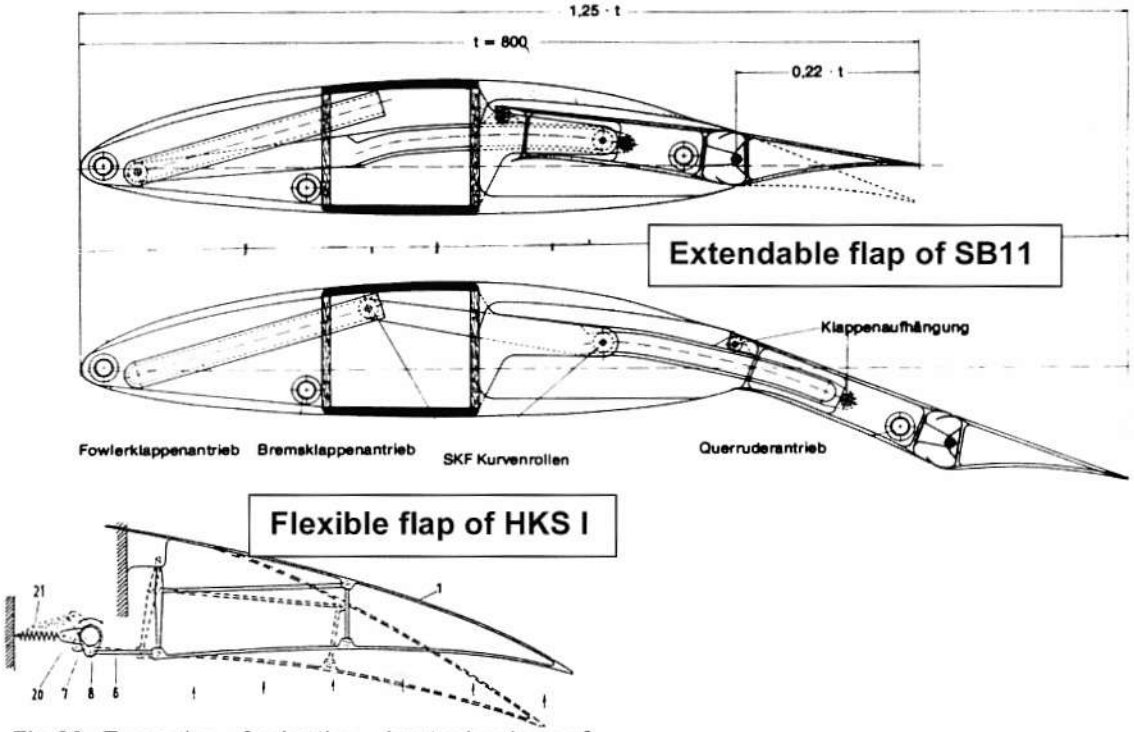

Fig 29: Examples of adaptive wing technology of gliders

FUTURE ASPECTS

Adaptive wing and morphing technologies are terms frequently used in papers and at meetings treating the improvement of recent aircraft configuration for military and civil application. Some of these technologies being in discussion are already tested on sailplanes. Several sailplanes have been equipped with a gapless flexible trailing edge flap: HKS I/III and SB 8 V2 in the sixties, Speed Astir in the eighties, (see figure 29) and Darmstadt D12 already in the thirties. Different types of gapless drag saving airfoil extensions in chord as well as in span direction have been constructed and flight tested by different Academic Flight Groups: SB 11 (see figure 29), Mü 27, D 40 , fs 32, all with chord extension and fs 29 with span extension. The result of all these attempts show, that the disadvantages of the respective configuration compensate or even overcompensate the advantages.

The blended wing body configuration (BWB) is the most favourite configuration of the future project offices of the aircraft industry. For the sailplane community this is an old hat. The Horten IV flew in 1941 and the SB 13 in 1988. Both have a small respectively a blended fuselage. They both achieved the performances of configurations with normal empennage at their time. But both need more attention of the pilot to control them which is a clear disadvantage.

The gain in performance of future sailplanes seems not to come from unusual configurations or morphing technologies. Perhaps it results from a number of small steps: The adaptation of airfoils to the lift and Reynolds number range for a specific configuration can be further improved. The sensitivity against insect contamination can be reduced for normal use in glider groups or can be neglected for competition sailplanes if the cleaning devices will be further improved. The blending range of wing and fuselage as well as of wing and winglet can be designed more accurately. Airfoils up to now are only tested at steady conditions but they fly at unsteady conditions. There should be a potential for further improvements too. In general the application of modern CFD methods for sailplane design and analysis could result in a potential for further improvements.

But perhaps one day W. Pfenningers dream comes true. He fought all his life for laminarisation by suction and one of his configurations was a fully laminar flow sailplain with an LoD above 100.

REFERENCES

[1] Brinkmann, G.; Zacher, H.: Die Evolution der Segelflugzeuge, Bernard & Graefe, Bonn, 1992

[2] Drela, M.,Youngren, H.: XFOIL User Guide Version 6.94, MIT Aero&Astro, 2001

[3] Eppler, R.:Airfoil Design and Data, Springer Verlag, Berlin, 1990

[4] Riegels, F.: Aerodynamische Profile, Oldenbourg Verlag, 1958

[5] Doetsch, H.: Untersuchungen an einigen Profilen mit geringem Widerstand im Bereich kleiner ca-Werte, Jb. 1940, dtsch. Luftfahrtforschung, Bd. I, S 54-57.

[6] Abbot, I.H., Doenhoff, A.E.: Theory of Wing Sections, Dover Publications, New York, 1949

[7] Althaus, D., Wortmann, F. X.: Stuttgarter Profilkatalog II, Vieweg, Braunschweig - Wiesbaden

[8] Horstmann, K. H.; Quast, A.; Boermans, L. M. M.:Pneumatic turbulators - A device for drag reduction, AGARD CP 365, Paper 20, 1984

[9] Horstmann, K. H.; Quast, A.: Widerstands-verminderung durch Blastubulatoren, DLR-FB 81-33, 1981

[10] Boermans, L.M.M., van Garrel, A.: Design and Wind Tunnel Test Results of a flapped Laminar Flow Airfoil for High-Performance Sailplane Applications, ICAS-94-5.4.3, 1994